Journal of
Synchrotron
Radiation

ISSN 0909-0495

Received 25 February 2008
Accepted 30 July 2008

Precise determination of elastic constants by high-resolution inelastic X-ray scattering

Hiroshi Fukui,[a,b]* Tomoo Katsura,[a] Takahiro Kuribayashi,[c] Takuya Matsuzaki,[a] Akira Yoneda,[a] Eiji Ito,[a] Yasuhiro Kudoh,[c] Satoshi Tsutsui[d] and Alfred Q. R. Baron[b,d]

[a]Institute for Study of the Earth's Interior, Okayama University, Japan, [b]Materials Dynamics Laboratory, SPring-8/Harima Institute, RIKEN, Japan, [c]Institute of Mineralogy, Petrology and Economic Geology, Tohoku University, Japan, and [d]Japan Synchrotron Radiation Research Institute, SPring-8, Japan. E-mail: fukuih@spring8.or.jp

Inelastic X-ray scattering (IXS) measurements have been performed on an MgO single crystal in order to evaluate IXS as a methodology for accurate and precise determination of elastic constants and sound velocities. By performing the IXS experiment using a 12-analyzer array, the complete set of single-crystal elastic constants of MgO were determined to a precision better than 0.8% (sound velocities to better than 0.2%). The results are consistent with values in the literature. The precision and accuracy of this work, which is significantly better than other published work to date, demonstrates the potential of IXS in determining elastic properties.

Keywords: inelastic X-ray scattering; elastic constants; sound velocity; single crystal; MgO; the Christoffel equation.

1. Introduction

Elasticity is a basic property of materials, indicating their strength and flexibility. There are several techniques to determine the elastic constants of materials by ultrasound (Jacobsen *et al.*, 2002; Oda *et al.*, 1994; Yoneda, 1990), but they usually require large samples (linear dimensions of a few hundred micrometres or more). However, large crystals of sufficient quality are not always available. Furthermore, most ultrasound techniques are not easily applied at pressures greater than 20 GPa (Higo *et al.*, 2008). Elasticity at higher pressures can be determined, in some cases, by other techniques. For example, Brillouin light scattering (BLS) can be applied to measure elastic constants of tiny crystals under pressure (Zha *et al.*, 2000), but it is difficult to apply to opaque materials. A related technique, impulsive stimulated light scattering (ISLS), can be applied to opaque materials under high-pressure conditions (Crowhurst *et al.*, 2004). However, using ISLS to study opaque materials under high-pressure conditions is complicated because it relies on probing the interface formed by the sample in contact with the pressure medium: the obtained bulk elastic properties depend on assumptions about the elastic properties of the material surrounding the sample. The mathematical treatment is also somewhat complicated. Another technique, nuclear resonant inelastic scattering, can provide the phonon density of states, from which an aggregate sound velocity can be determined, but it is difficult to obtain elastic constants using this method. It is also limited to samples which contain Mössbauer nuclei.

Inelastic X-ray scattering (IXS) is a technique for obtaining elastic constants from samples since the measured sound velocity, as the wavenumber approaches zero, corresponds to that of the elastic wave. Since X-ray beams may be focused to spot sizes of a few tens of micrometres, this technique can be applied to similarly sized samples. As hard X-rays are penetrating, it can also be applied to samples within more complex environments, such as diamond-anvil cells. Since it is possible to obtain structural information on the same instrument, the ambiguity of dimension parameters can be reduced. Also, of course, the X-ray determination is independent of optical opacity of the samples. Inelastic neutron scattering (INS), which can provide similar information in principle, requires much larger samples ($\gg 10$ mm^3).

There are only a limited number of reports treating the determination of elastic constants with IXS (Antonangeli *et al.*, 2004; Bosak *et al.*, 2006, 2007) and the precision of the determination varies from several percent to >10%. This level of precision does not give sufficiently precise values for geophysical application. For example, laboratory results on sound velocities of candidate materials in the earth's interior are used for estimation of the temperature structure. In the case of MgO, the temperature dependence of longitudinal sound velocity is -6×10^{-4} km s^{-1} K^{-1} (Isaak *et al.*, 1989). A 5% error in the sound velocity (0.5 km s^{-1}) corresponds to 800 K.

In this paper we present an experimental determination of the elastic constants of magnesium oxide using high-resolution IXS. Since the elasticity of MgO has been extensively studied,

we can compare our results against well known literature values and demonstrate the capability of IXS. The IXS data have been collected at arbitrary momentum transfers, not only along high-symmetry crystallographic directions, which matched a multi-analyzer IXS spectrometer and made the experiment highly efficient. The accuracy and precision of the elastic property determination will be discussed.

2. Experimental

The IXS experiment was carried out at BL35XU at SPring-8 (Baron *et al.*, 2000). The energy of the incident beam and the energy resolution were 21.747 keV and ~1.5 meV full width at half-maximum (FWHM) using the Si (11 11 11) reflection. We used a 3 × 4 array of spherical analyzer crystals at the end of the 10 m horizontal arm to analyze the scattered X-rays with 12 different scattering vectors (Baron *et al.*, 2008). The dimension of the incident X-ray beam in the present work was about 100 μm diameter (FWHM), but can be reduced to smaller sizes when required (~20 μm). Energy scans (at constant momentum transfer) were carried out by changing the energy of the X-rays incident on the sample by thermal expansion of the backscattering monochromator crystal, while the energy (temperature) of the analyzers was held fixed.

The energy scale was determined using the temperature-dependent thermal expansion of silicon (Lyon *et al.*, 1977) ($\alpha_{\rm silicon} = 2.6453 \times 10^{-6}\ {\rm K}^{-1}$ at the elastic peak at 303.12 K) calibrated, in the present set-up, using a known phonon in diamond (Kulda *et al.*, 2002). The temperature variation of the thermal expansion parameter of silicon is relatively weak (0.3% K^{-1}) and was not a serious source of error, since the temperatures used in the experiment were stable to better than 10 mK and reproducible. Given our use of the Stokes–anti-Stokes separation to determine the phonon energy, the important contributions to error in the energy scale are (i) possible instabilities on the time scale of a single scan and (ii) the systematic error in the calibration. Comparison of the elastic peak position in successive scans suggests that the stability of the energy-temperature scale was better than ±0.2 meV. The systematic error in the calibration is more difficult to quantify. The longitudinal optical mode of diamond was taken to have an energy of 164.7 meV at Q = (1.1 1.1 1.1) from Kulda *et al.* (2002). The agreement achieved in that work between three estimates of phonon energy [164.67 ± 0.31 (INS), 164.69 ± 0.03 (IXS) and 164.71 (local density approximation) is extremely good. However, the accuracy of the value is not clear, with the only comment being that the INS scale is probably not reliable to better than 1–2 meV. Meanwhile, experience with the set-up used in the present measurement means that when we are most careful in our temperature scale (calibration, attachment, thermal shielding of sensors) the agreement with the 164.7 meV value is within 0.5% of the measured energy based on the thermal expansion data of Lyon *et al.* (1977). We then take our energy scale, after calibration, to have a systematic error of less than 0.5%.

The sample was a commercial single crystal of MgO of 1.0 mm thickness bought from Tateho Chemical Industries. The sample was set, in air, on the Eulerian cradle of the IXS spectrometer. The lattice parameter of this crystal was measured off-line (laboratory source) and found to be 4.212 Å. After placement on the IXS spectrometer, four reflections (and the previously measured lattice constants) were used to determine the orientation matrix (UB matrix). The measured mosaic spread of the (4 0 0) reflection was 0.024°. Measurements were made near to the (4 0 0) and (2 $\bar{2}$ 0) Bragg reflections with momentum resolutions set to (0.024 0.025 0.007) and (0.024 0.024 0.005) full width, respectively. It took about 17 h to obtain all of the spectra used in the analysis presented here.

3. Analysis

Fig. 1 shows a representative set of 12 IXS spectra obtained, simultaneously, using the 12-analyzer array. Generally, the spectra consist of several pairs of lines (each pair being a Stokes and an anti-Stokes excitation of one mode) in addition to an elastic contribution near zero energy transfer. Up to three pairs of acoustic modes can in principle occur at any given momentum transfer. In previous work, IXS spectra were typically measured along high-symmetry directions where only one pair of lines was visible in order to simplify the analysis. Since all of 12 analyzers cannot be located under such conditions simultaneously, multiple pairs of Stokes and anti-Stokes lines are seen in some spectra. Because most spectra were measured almost at points with high symmetry in reciprocal space, one of the transverse modes was not detected. At small reduced momentum transfer, in principle three modes can appear but generally two transverse modes are almost degenerated. Pseudo-Voigt functions were used to fit the peaks shown in a spectrum by least-squares methods. One of the fit spectra is shown in Fig. 2.

The energy zero for each spectrum was determined from the average value of Stokes and anti-Stokes peaks. While the elastic peak might be used, it is essentially a dirt effect, typically resulting from imperfections in the sample, and/or scattering from the sample environment. In particular, elastic scattering from the sample environment, for which the source point can be different than the centre of the spectrometer, can occur at an energy slightly shifted from the elastic value for the sample in the centre of the spectrometer. Thus, the centre of the Stokes–anti-Stokes pair, when available, is the best determination of the energy zero.

For precise determination of elastic constants using the multi-analyzer IXS spectrometer, we used not only data along high-symmetry directions but also those at arbitrary points in reciprocal space. In order to calculate elastic constants from measured energies and momentum transfers of phonons, we used the Christoffel equation (p. 211 of Auld, 1973),

$$\rho\,(\omega/|\mathbf{q}|)^2\mathbf{A} = \mathbf{ChA}, \qquad (1)$$

where ρ, ω, $|\mathbf{q}|$ and $\mathbf{A}$ are the density of the sample, angular frequency, wavevector and polarization vector (or amplitude) of the plane elastic wave, respectively. **Ch** is a 3 × 3 matrix, the elements of which are

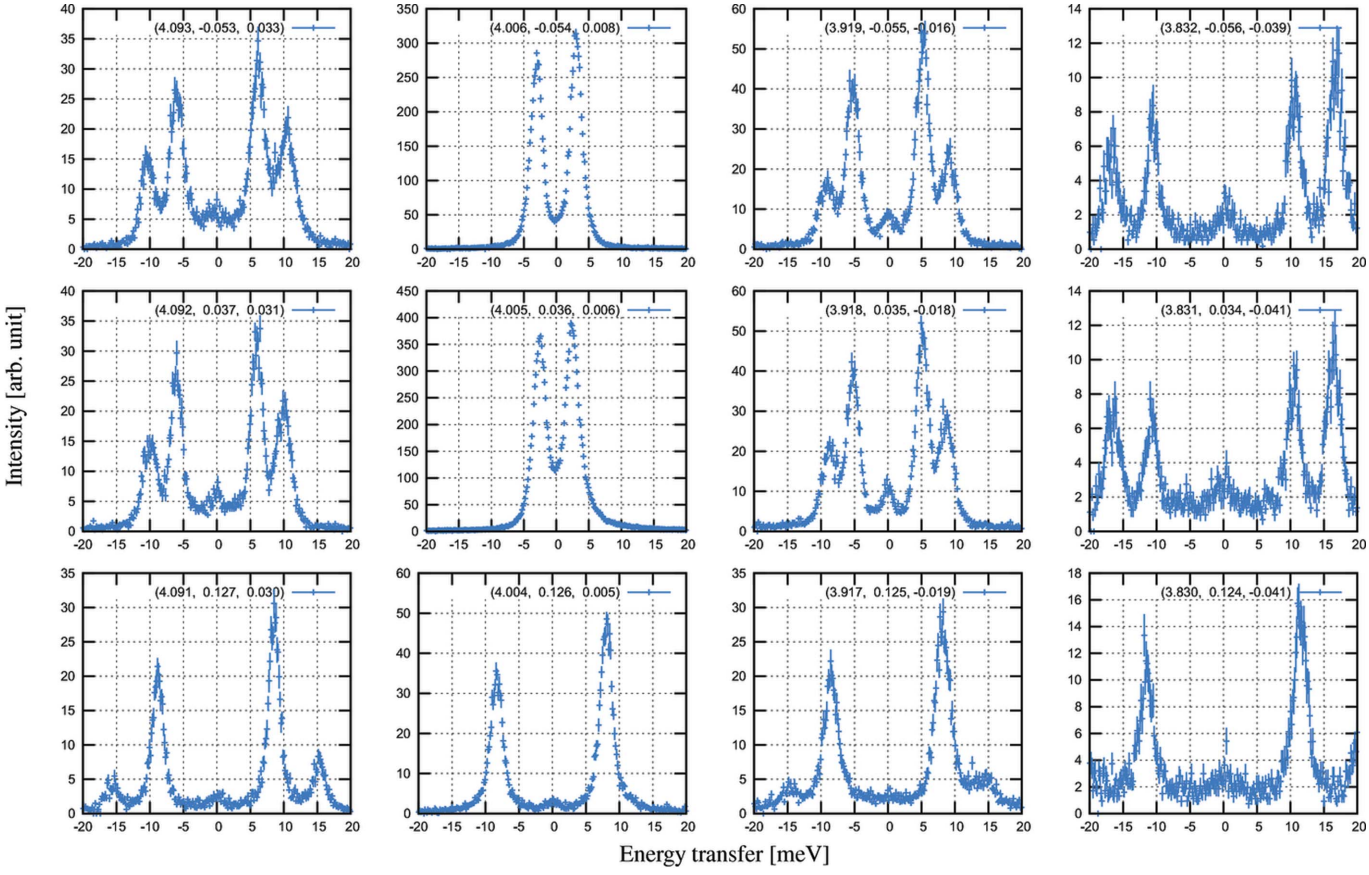

Figure 1
Representative IXS spectra of a single crystal of MgO obtained using the 12-analyzer IXS spectrometer. The reciprocal lattice coordinate of the spectrometer-arm centre is (3.962, 0.036, −0.006) in reciprocal lattice units (r.l.u.). The reciprocal lattice coordinate of each analyzer is shown in the figure.

$$\mathrm{Ch}_{11} = C_{11}n_1^2 + C_{66}n_2^2 + C_{55}n_3^2 + 2(C_{16}n_1n_2 + C_{56}n_2n_3 + C_{15}n_3n_1),$$

$$\mathrm{Ch}_{22} = C_{66}n_1^2 + C_{22}n_2^2 + C_{44}n_3^2 + 2(C_{26}n_1n_2 + C_{24}n_2n_3 + C_{46}n_3n_1),$$

$$\mathrm{Ch}_{33} = C_{55}n_1^2 + C_{44}n_2^2 + C_{33}n_3^2 + 2(C_{45}n_1n_2 + C_{34}n_2n_3 + C_{35}n_3n_1),$$

$$\mathrm{Ch}_{12} = \mathrm{Ch}_{21} = C_{16}n_1^2 + C_{26}n_2^2 + C_{45}n_3^2 + (C_{12} + C_{66})n_1n_2 + (C_{25} + C_{45})n_2n_3 + (C_{14} + C_{56})n_3n_1,$$

$$\mathrm{Ch}_{23} = \mathrm{Ch}_{32} = C_{56}n_1^2 + C_{24}n_2^2 + C_{34}n_3^2 + (C_{25} + C_{46})n_1n_2 + (C_{23} + C_{44})n_2n_3 + (C_{36} + C_{45})n_3n_1,$$

$$\mathrm{Ch}_{31} = \mathrm{Ch}_{13} = C_{15}n_1^2 + C_{46}n_2^2 + C_{35}n_3^2 + (C_{14} + C_{56})n_1n_2 + (C_{36} + C_{45})n_2n_3 + (C_{13} + C_{55})n_3n_1,$$

where C_{ij} are elastic stiffness constants and (n_1, n_2, n_3) indicates the propagation vector (direction vector of **q**) in a Cartesian coordinate system. In the case of a cubic material, **Ch** is rewritten using the relationship between the elastic constants [$C_{11} = C_{22} = C_{33}$, $C_{44} = C_{55} = C_{66}$, $C_{12} = C_{23} = C_{31}$, and the others are zero (see p. 362 of Auld, 1973)] as

$$\mathbf{Ch}_{\mathrm{cubic}} = \begin{bmatrix} C_{11}n_1^2 + C_{44}(n_2^2 + n_3^2) & (C_{12} + C_{44})n_1n_2 & (C_{12} + C_{44})n_3n_1 \\ (C_{12} + C_{44})n_2n_1 & C_{11}n_2^2 + C_{44}(n_3^2 + n_1^2) & (C_{12} + C_{44})n_2n_3 \\ (C_{12} + C_{44})n_3n_1 & (C_{12} + C_{44})n_2n_3 & C_{11}n_3^2 + C_{44}(n_1^2 + n_2^2) \end{bmatrix}. \quad (2)$$

The density of the samples was calculated from the lattice parameter and the total weight of the atoms in the unit cell. The elastic constants can be obtained by solving the eigenvalue problem for the **Ch** matrix. The elastic constants C_{ij} were taken as fitting parameters and a least-squares algorithm was used to minimize the difference between the measured phonon frequencies and those found from inverting the eigenvalue problem of equation (1). In addition, we adopted an *hkl* correction vector, $(\Delta h\ \Delta k\ \Delta l)$, as a fitting parameter to eliminate possible effects from systematic errors in alignment [*e.g.* $(h\ k\ l)_{\mathrm{real}} = (h\ k\ l)_{\mathrm{nominal}} + (\Delta h\ \Delta k\ \Delta l)$], as will be discussed in more detail below. Thus, six free parameters [three elastic constants, and three components $(\Delta h\ \Delta k\ \Delta l)$] were used to fit 172 data points.

We included a correction to the mode energies owing to the finite Q-resolution. For ideal Q-resolution, the intensity of inelastic scattering by acoustic phonon, I, can be expressed as the following equation: $I \propto q^{-2}$, where q is a reduced momentum transfer. Here we assume that the phonon signal is δ-function-like at $E = E_0$ and that the phonon dispersion is

Table 1
Elastic moduli and sound velocities of MgO.

A: present result; B: Isaak *et al.* (1989); C: Yoneda (1990); D: Oda *et al.* (1994); E: Sinogeikin & Bass (1999); F: Zha *et al.* (2000); G: Jacobsen *et al.* (2002). IXS: inelastic X-ray scattering; RPR: rectangular parallelepiped resonance; UI: ultrasonic interferometry; RSUS: resonant sphere ultrasound spectroscopy; BLS: Brillouin light scattering.

Method	A IXS†	B RPR	C UI	D RSUS	E BLS	F BLS	G UI
C_{11} (GPa)	293.9 ± 1.0	298.96 ± 0.65	297.8	296.03 ± 0.13	297.9 ± 1.5	–	298 ± 2
C_{12} (GPa)	95.2 ± 0.7	96.42 ± 0.61	95.1	95.35 ± 0.13	95.8 ± 1.0	–	92 ± 5
C_{44} (GPa)	154.9 ± 0.2	157.13 ± 0.31	155.8 ± 0.15	155.89 ± 0.05	154.4 ± 2.0	–	157 ± 2
K_S (GPa)	161.4 ± 0.6‡	163.93 ± 0.60	162.7 ± 0.2	162.13 ± 0.12	163.2 ± 1.0	162.5 ± 0.7	160 ± 3
G_S (GPa)	129.6 ± 0.3‡	131.8 ± 0.5§	131.1 ± 0.1‡¶	130.68 ± 0.05‡¶	130.2 ± 1.0	130.4 ± 1.7	133 ± 2
V_L (km s^{-1})	9.656 ± 0.011	9.73 ± 0.01	9.702 ± 0.002¶	9.682 ± 0.004¶	9.69 ± 0.03¶	9.68 ± 0.04	9.70 ± 0.04¶
V_T (km s^{-1})	6.013 ± 0.008	6.06 ± 0.01	6.048 ± 0.002¶	6.034 ± 0.002¶	6.03 ± 0.03¶	6.06 ± 0.03	6.08 ± 0.04¶

† Sound velocities and elastic constants have a systematic uncertainty of 0.5 and 1.0%, respectively, owing to energy calibration (see text). ‡ Voight–Reuss–Hill average. § Hashin–Shtrikman average. ¶ Calculated values using elastic constants and their errors.

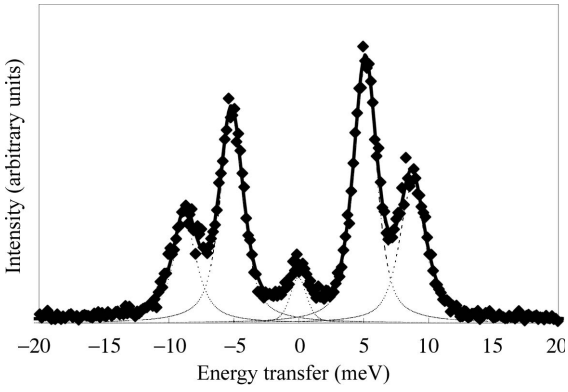

Figure 2
The third left spectrum in the middle row of Fig. 1 (solid diamonds) with the best-fit result using pseudo-Voigt functions (thin dotted lines for the individual components and thick solid line for the total fit).

linear, $E = \alpha q$. In this case, the obtained signal intensity varies with q and therefore with E. Consequently, the centroid of the obtained signal can be different from the true centre E_0. The centroid can be calculated using the following equation,

$$E_{\rm centroid} = \frac{\int_{E_1}^{E_2} EI(q)\,{\rm d}E}{\int_{E_1}^{E_2} I(q)\,{\rm d}E} = \frac{\alpha}{\Delta q}\left(q_0^2 - \frac{\Delta q^2}{4}\right)\ln\left[\frac{q_0 + (\Delta q/2)}{q_0 - (\Delta q/2)}\right]$$
$$\simeq \alpha q_0\left[1 - \frac{1}{6}\left(\frac{\Delta q}{q_0}\right)^2 + \ldots\right],$$

where q_0 is the momentum transfer at $E = E_0$ and Δq is the Q-resolution. Therefore, $\Delta E = E_0 - E_{\rm centroid}$ is the value for the energy correction. Using lattice constants and (h k l) values obtained without energy correction, we calculated ΔE for all measured phonons assuming the obtained phonon energies without energy correction as E_0, which is appropriate as the first approximation. In the end, the six parameters were optimized using the corrected energy values. The values of the energy correction are shown in Fig. 3. We used 0.025 r.l.u. as Δq for all measured points. Note that we assume that Δq is much smaller than q_0 and an energy gradient exists along the propagating direction. In the case that Δq is comparable with measured q_0, one must consider a more complicated correction owing to the energy gradients perpendicular to the propagating direction.

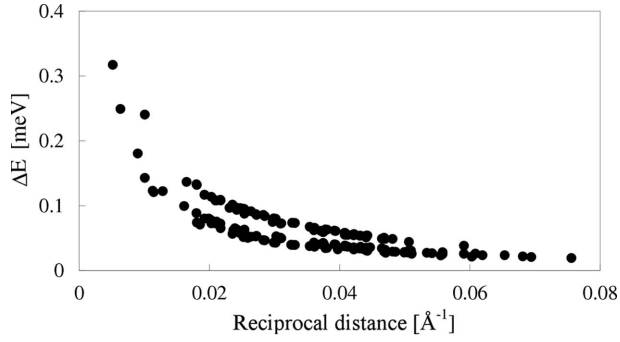

Figure 3
Values of the energy correction originating from finite Q-resolution. The correction is the larger at the point closer to the Γ point.

4. Results

The obtained elastic constants and sound velocities with the corrections are shown in Table 1. Adiabatic bulk and shear moduli K_S and G_S have been calculated from the elastic constants. Aggregate sound velocities of compressional (longitudinal) and shear (transverse) waves V_L and V_T calculated from K_S, G_S and the density are also listed.

Figs. 4 and 5 show the residues of the observed phonon energies from those obtained by fitting with and without the corrections, respectively. The residues are plotted in (*a*) against the absolute values of the reduced momentum transfers $\mathbf{q}$, which is expressed as $\mathbf{Q} = \boldsymbol{\tau} + \mathbf{q}$, where $\mathbf{Q}$ is the total momentum transfer and $\boldsymbol{\tau}$ is the reciprocal lattice vector nearest to $\mathbf{Q}$. This type of plot will show the divergence from the linear dispersion (see *Discussion*). The residues are also plotted against the projected momentum transfer to each axis in (*b*), (*c*) and (*d*), which will show the possible errors in alignment. It is seen that the residues are reduced by the *hkl* correction, which drastically improved the precision of determination of elastic constants. The *hkl* correction vector was found to be (0.0056 ± 0.0005, −0.0080 ± 0.0007, 0.0043 ±

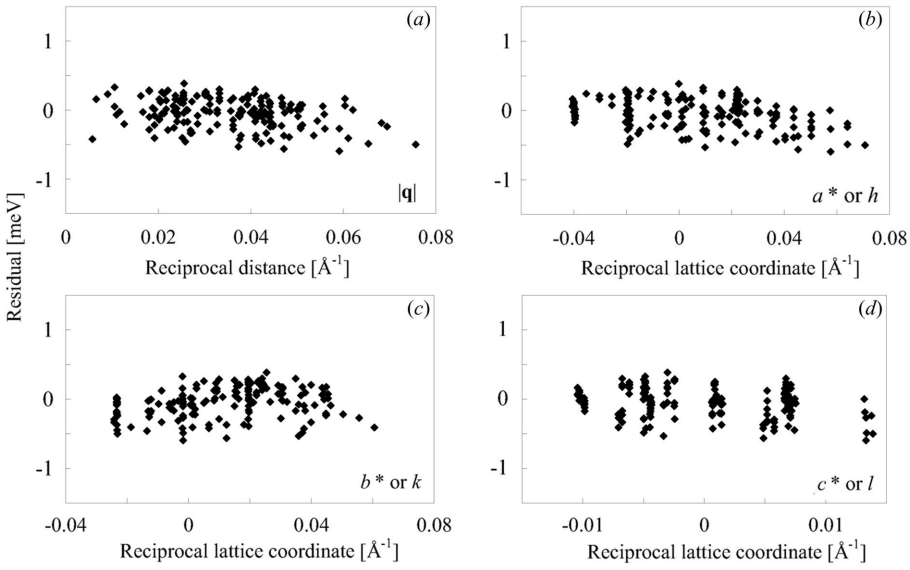

Figure 4
Residues of the fit to the phonon energies *versus* (*a*) reciprocal distances and against (*b*, *c*, *d*) reciprocal lattice coordinates of *a**, *b** and *c**, respectively. The *hkl* correction vector is [0.0056 (5), −0.0080 (7), 0.0043 (12)] in r.l.u. The reliability factor is 1.67%.

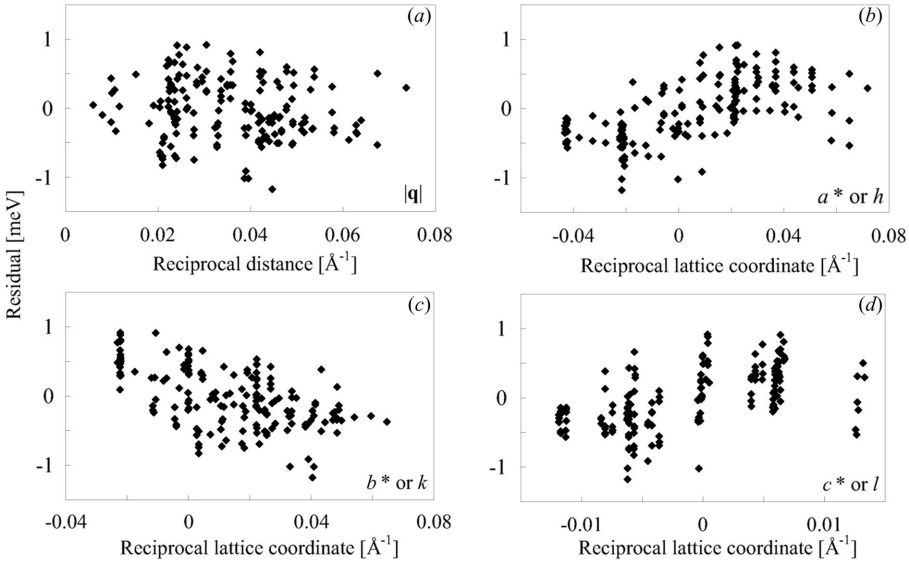

Figure 5
Residues of the fit to the phonon energies without the *hkl* and energy corrections *versus* (*a*) reciprocal distances and against (*b*, *c*, *d*) reciprocal lattice coordinates of *a**, *b** and *c**, respectively. The residues seem to be correlated with *a**, *b** and *c**. The reliability factor is 3.46%.

0.0012) in r.l.u., which corresponds to angular misalignment of about 0.1°. The errors in elastic constants are found to decrease by one order of magnitude using the correction. For example, the value of C_{11} changes from 288 ± 5 GPa to 293.9 ± 1.0 GPa. Defining the reliability factor as

$$\sum \left| E_{\rm obs} - E_{\rm calc} \right| / \sum E_{\rm obs},$$

where $E_{\rm obs}$ and $E_{\rm calc}$ are the phonon energy from the observation and model, respectively, we see this factor improved from 3.46% to 1.67% when the *hkl* correction is included.

It should be noted that there can be two different origins for the *hkl* correction used here. One is the misalignment of the sample, corresponding to an error in the UB matrix used during the experiment. Another is the misalignment of the spectrometer. In particular, IXS instruments usually require focusing and other optics, so the incident beam is not horizontal but slightly off horizontal; for the present spectrometer, and set-up, the beam was incident at about 3.5 mrad off horizontal. Meanwhile, the spectrometer 2θ arm moves in the horizontal plane, so there are almost always small systematic errors. The magnitude of this error will depend upon precisely how the UB matrix is determined, but, to a first approximation, can be considered a constant offset in the neighbourhood of any fixed reciprocal lattice point. Thus the correction introduced here is a convenient way to account for these sources of error, while taking advantage of the fact that relative motions of the spectrometer are extremely precise.

5. Discussion

The results of the elastic constants and velocities of MgO determined by different techniques are shown in Table 1 (Isaak *et al.*, 1989; Yoneda, 1990; Oda *et al.*, 1994; Sinogeikin & Bass, 1999; Zha *et al.*, 2000; Jacobsen *et al.*, 2002). The previous studies give the compressional and shear wave velocities of 9.68–9.73 and 6.03–6.08 km s^{-1}, respectively. Despite the difference in methods, the results of those studies are in excellent agreement. The compressional and shear wave velocities obtained in the present work are 9.656 and 6.013 km s^{-1}, respectively. Although the present values are slightly smaller than the lower limit of the above ranges, the difference from the intermediate values are only 0.5–0.7%. Thus IXS is an accurate method for determining elastic constants.

Note that the compressional and shear velocities obtained without the corrections are 9.48 and 5.85 km s^{-1}, which are out of the above range. The *hkl* correction vector determined through the fitting was small but improved the accuracy and precision of the determination. This means the small deviation of measured **q** from the assumed direction causes large errors. Consequently the crystal orientation should be carefully determined and all the measurements should be completed at

one attempt without dismounting the sample from the spectrometer.

The present method has determined the elastic constants and velocities of MgO with 0.2–0.7% and 0.1–0.2% of errors, respectively. This precision favourably compares with those of the other techniques. The errors in the determination of elastic properties with IXS in the previous studies were a few percent in bulk modulus (Antonangeli *et al.*, 2004; Bosak *et al.*, 2006, 2007), which are larger than the present one (0.4%) by more than one order of magnitude. In this study we assigned one phonon energy measured at a certain **q** with one corresponding sound velocity propagating to the direction by using equations (1) and (2) within the approximation of linear dispersion. The multi-analyzer IXS spectrometer yields the large number of data in a limited time, which leads to very precise results.

There is a concern as to whether the dispersion of the acoustic modes is truly linear in the measured region of reciprocal space. In the previous studies (Bosak *et al.*, 2006, 2007), a sinusoidal function was used to fit phonon energies measured along a high-symmetry direction to help compensate for this problem. In our work the deviation from linear dispersion would appear as a negative correlation between the fitting residues and the reciprocal distances in a plot like Fig. 4(*a*) as has been seen in another case (Fukui *et al.*, 2008). The present case shows a very weak negative correlation between the reciprocal distance and the residue (the correlation coefficient is −0.297). If the correlation was large, a cut-off $|\mathbf{q}|$ value could be set to improve the fitting results and the analysis performed with only the data points measured at a reciprocal distance smaller than the cut-off. It might also be better to choose a momentum-dependent cut-off taking the shape of the Brillouin zone into account. It is obviously preferable that the IXS spectra are measured as close to a Γ-point as possible, given constraints owing to sample quality and momentum resolution (However, note that it is not always better to measure an IXS spectrum at the point closer to a Γ-point since the effect of finite Q-resolution on the observed phonon energy is larger as shown in Fig. 3.) In the present case the large number of data points in the range $0.02 < |\mathbf{q}| < 0.03$ Å^{-1} efficiently constrained the values of the elastic constants, giving small errors in spite of relatively scattered residues shown in Fig. 4(*a*).

Another good point of the present method is the use of the energies of phonons propagating in arbitrary directions. The velocities $V_{\mathrm{L}[100]}$ and $V_{\mathrm{T}[100]}$ are only related to C_{11} and C_{44}, respectively. Since sound velocities propagating in arbitrary directions are complicated functions including all elastic stiffness constants, the data points obtained at arbitrary points constrain all of the elastic constants in relatively equal measure and prevent an excessive error on a certain constant, *e.g.* C_{12} in this case, owing to the error propagation.

In general, mosaicity of the sample could be a significant source of error, though the present sample has a low mosaic spread. A sample with large rocking-curve widths sometimes gives an inconsistent UB matrix. Thus a reasonably good crystal is important, and at higher pressures one should try to maintain hydrostatic conditions to reduce induced strain

6. Summary

We have determined the elastic constants of MgO by IXS. The use of an analyzer array and the Christoffel equation to analyze data along arbitrary directions in reciprocal space allows unprecedented precision and accuracy for this technique, comparable with desired levels for geophysical applications. The careful examination of error correlations and a correction to account for sample and spectrometer misalignment is crucial to obtain both precise and accurate results.

We thank Taku Tsuchiya for his helpful comments. The synchrotron radiation experiments were performed with the approval of the Japan Synchrotron Radiation Research Institute (proposal No. 2006A1242). This work was supported by Grants-in-Aid for Young Scientists of Japan Society for the Promotion of Science and by the 21st century COE program at the Institute of Study of the Earth's Interior, Okayama University, Japan.

References

Antonangeli, D., Krisch, M., Fiquet, G., Farber, D. L., Aracne, C. M., Badro, J., Occelli, F. & Requardt, H. (2004). *Phys. Rev. Lett.* **93**, 215505.

Auld, B. A. (1973). *Acoustic Fields and Waves in Solids*, Vol. 1. Malabar: Krieger.

Baron, A. Q. R., Sutter, J. P., Tsutsui, S., Uchiyama, H., Masui, T., Tajima, S., Heid, R. & Bohnen, K.-P. (2008). *J. Phys. Chem. Solids.* To be published.

Baron, A. Q. R., Tanaka, Y., Goto, S., Takeshita, K., Matsushita, T. & Ishikawa, T. (2000). *J. Phys. Chem. Solids*, **61**, 461–465.

Bosak, A., Krisch, M., Mohr, M., Maultzsch, J. & Thomsen, C. (2007). *Phys. Rev. B*, **75**, 153408.

Bosak, A., Serrano, J., Krisch, M., Watanabe, K., Taniguchi, T. & Kanda, H. (2006). *Phys. Rev. B*, **73**, 041402R.

Crowhurst, J. C., Goncharov, A. F. & Zaug, J. M. (2004). *J. Phys. Condens. Matter*, **16**, S1137–S1142.

Fukui *et al.* (2008). In preparation.

Higo, Y., Inoue, T., Irifune, T., Funakoshi, K.-I. & Li, B. (2008). *Phys. Earth Planet. Inter.* **166**, 167–174.

Isaak, D. G., Anderson, O. L. & Goto, T. (1989). *Phys. Chem. Miner.* **16**, 704–713.

Jacobsen, S. D., Reichmann, H.-J., Spetzler, H. A., Mackwell, S. J., Smyth, J. R., Angel, R. J. & McCammon, C. A. (2002). *J. Geophys. Res.* **107**(B2), 2037.

Kulda, J., Kainzmaier, H., Strauch, D., Dorner, B., Lorenzen, M. & Krisch, M. (2002). *Phys. Rev. B*, **66**, 241202.

Lyon, K. G., Salinger, G. L., Swenson, C. A. & White, G. K. (1977). *J. Appl. Phys.* **48**, 865.

Oda, H., Isoda, S., Inouye, Y. & Suzuki, I. (1994). *J. Geophys. Res.* **99**, 15517–15527.

Sinogeikin, S. V. & Bass, J. D. (1999). *Phys. Rev. B*, **59**, R14141.

Yoneda, A. (1990). *J. Phys. Earth*, **38**, 19–55.

Zha, C.-S., Mao, H.-K. & Hemley, R. J. (2000). *Proc. Natl. Acad. Sci.* **97**, 13494–13499.